

Figure 2.9: SST based on an 8 days average from AVHRR Pathfinder for the end of June 1996.

Eastern Region: Robe to Tasmania

Off the northwest coast of Tasmania Baines et al. (1983) used a single transect of temperature to infer the existence of the ZC. Subsequent current meter and CTD observations during 1988 (Lyne and Thresher, 1994) show that the current during this year had a persistent southward flow with speeds exceeding 50 cm s^{-1} at depths of 200 m. At the 2000 m isobath and for the depth of $\sim 1000 \text{ m}$, a northward current reaching values of more than 10 cm s^{-1} was found. Subsequent Acoustic Doppler Current Profiler (ADCP) observations taken near the same site, but during 1997-1998 (Cresswell, 2000), show that the current can be much weaker with values generally smaller than 30 cm s^{-1} in 200 m of water. With the purpose of evaluating the mean monthly and seasonal currents, both data sets were re-examined in Chapter 6. Surface drift bottles, card data and satellite-drifters (Newell, 1961; Lyne and Thresher, 1994; Cresswell, 2000)

poleward East Australian Current (EAC) flow along the eastern coast of Tasmania (that should not be confused with the Tasman Front, where the main branch of the EAC leaves the coast at latitudes of 35°S (e.g. Tomczak and Godfrey, 1994; Ridgway and Godfrey, 1997)). Indeed, according to Cresswell (2000), the position of this confluence is modulated by the strength of the ZC and EAC. The scenario described above can be identified in the monthly average composition of the SST images for the beginning of winter (Fig. 2.11). Here the two southward flows (the narrow and relatively warm ZC along the western Tasmanian coast and the broader and also warmer south branch of the EAC along the eastern coast of Tasmania) and the confluence zone are identified.

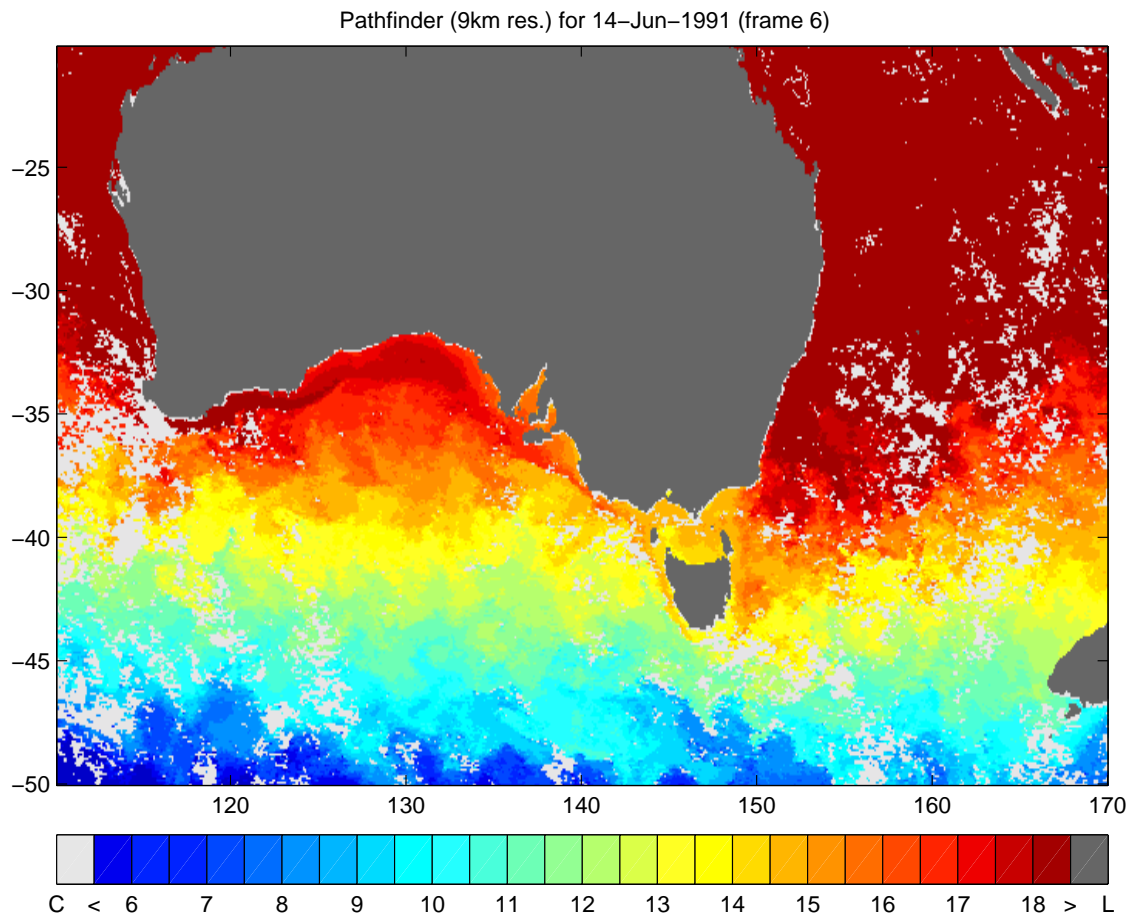


Figure 2.11: Same as Fig. 2.9, but using a monthly average for June, 1991.

Finally, the OCCAM section taken at the southern tip of Tasmania (Fig. 2.10c) illustrates the eastward ZC near the coast and westward inflow by the Tasman Outflow (Rintoul and Sokolov, 1999) at greater depths and farther offshore. The results for density (Fig. 2.10d) are very similar to the sectional data obtained by Rintoul and Bullister (1999) and shown here in Fig. 2.12: a 400-500 m deep SML exists, deep downwelling occurs

they produce excessive convection. In fact, it is most probably, that the final answer is a combination of these two reasons. Otherwise, the reproduction of dense water near the coast as indicated by Fig. 5.1a and CARS data (Fig. 2.4c) would not be found.

5.2 Effect of Enhanced Bottom Friction Through CTW and Tides

Periodic motions, such as CTWs and tides, can have an influence on the mean flow through enhanced bottom friction. In order to evaluate that, the basic case was rerun using the bottom stress formulation described in section 3.2.2, where $\tau_b = \rho_0 C_d \mathbf{u} (|\mathbf{u}|^2 + 2\sigma^2_{CTW} + 2\sigma^2_{TIDES})^{1/2}$, with σ being the *rms* of the bottom speed of the associated motion. For the tides, σ_{TIDES} was obtained from a tidal model described in Platov and Middleton (2000), while for the CTWs, σ_{CTW} was obtained from an idealised CTW model described in Appendix D. This experiment was named experiment 2 (Table 3.1).

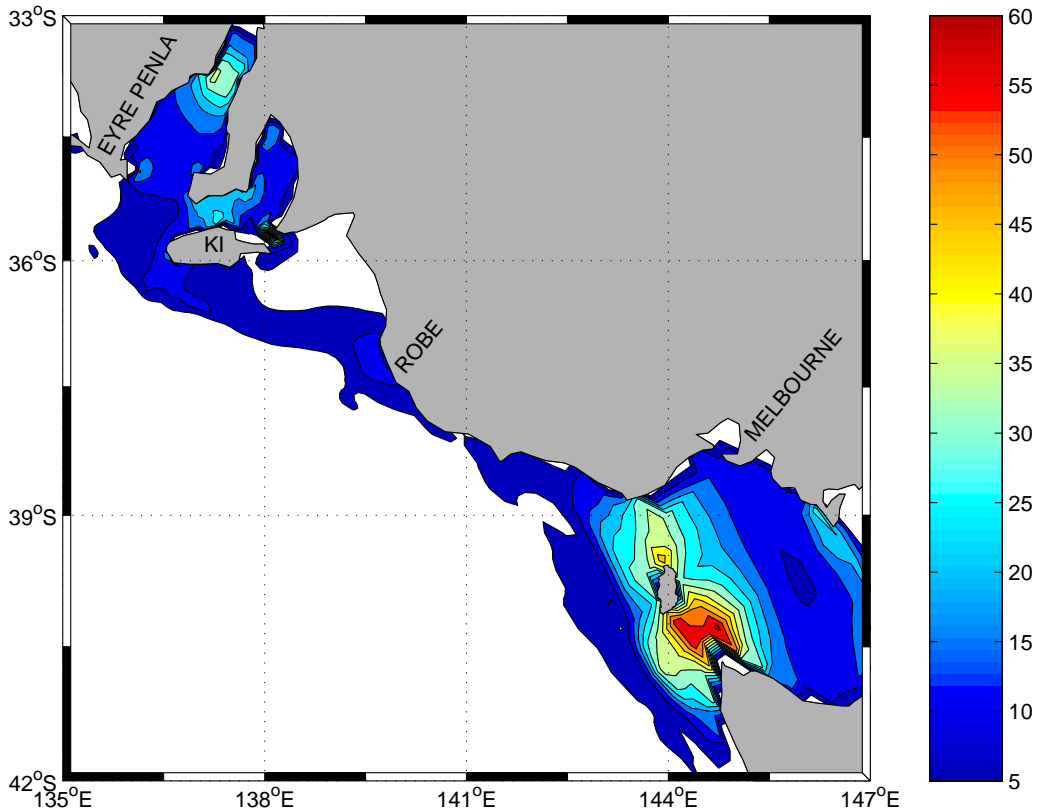


Figure 5.3: σ_{TIDES} as a sum of the K1, M2, O1 and S2 tidal constituents. The contour interval is 5 cm s^{-1} .

The ENSO index is presented in Fig. 6.13 and the two current meter data sets examined in section 6.1 were obtained during the year of 1988 (one of the largest La Niñas of the last 30 years) and the years 1997-1998 (a strong El Niño event). In both cases abnormally high and low sea level perturbations of order of 5 cm might be expected. Now, from the plots of west Tasmanian sea level (Fig. 4.19b) and alongshore velocity (Fig. 4.20b), a sea level difference of 5 cm between the coast and 1000 m isobath leads to a poleward current of up to 20 cm s^{-1} .

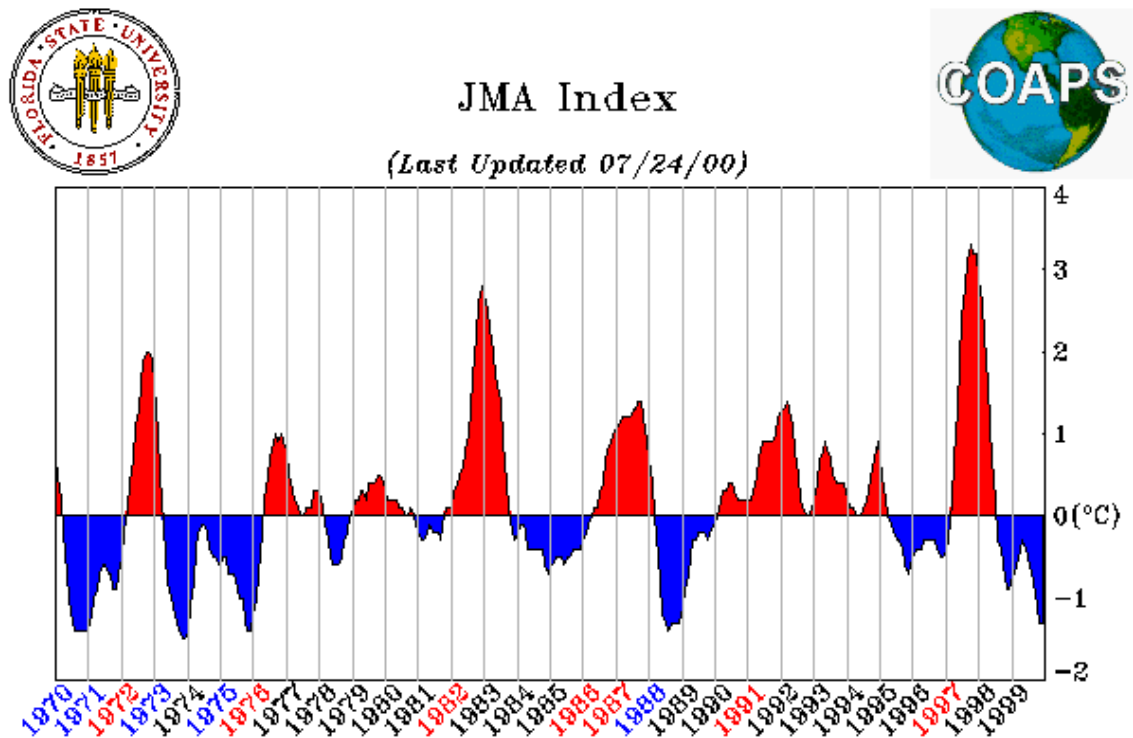


Figure 6.13: ENSO Index according to the Japan Meteorological Agency (JMA). The index is a 5-month running mean of spatially averaged SST anomalies over the tropical Pacific: 4°S - 4°N , 150°W - 90°W . El Niño years or warm events are represented in red labels while La Niña years or cold events are represented in blue labels. (extracted from [ftp : //www.coaps.fsu.edu/pub/JMA_SST_Index/jma.gif](ftp://www.coaps.fsu.edu/pub/JMA_SST_Index/jma.gif)).

For the ENSO signal, the offshore scale for sea level should scale with that of the low mode Rossby waves (Clarke and Van Gorder, 1994) and be of order of $\beta c_j^2 / \omega f^2$. For $c_1 = 3 \text{ m s}^{-1}$, $f = 10^{-4}$, $\beta = 2.0 \times 10^{-11}$ and $\omega = 2 \pi / (3 \text{ years})$, the above scale is close to 260 km. The associated alongshore geostrophic velocity for a 5 cm change in η is then only 2 cm s^{-1} .

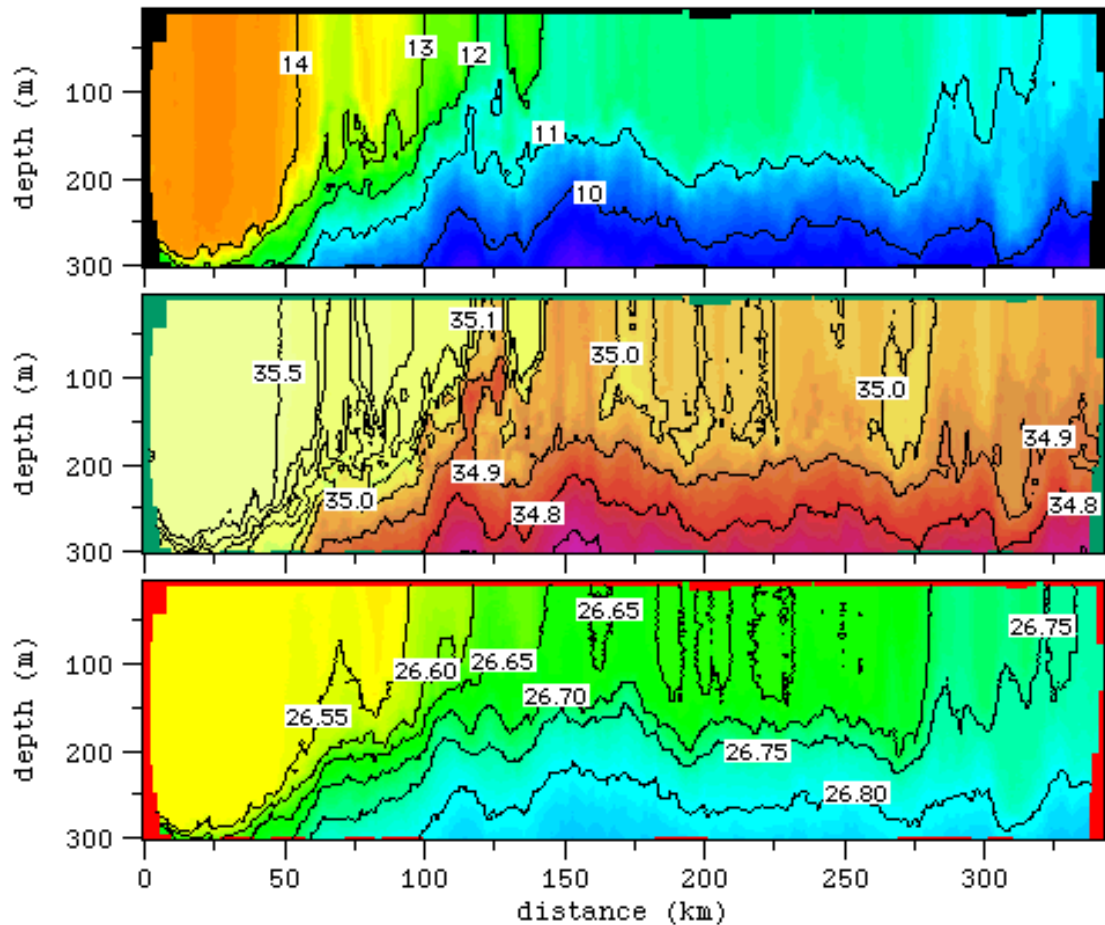


Figure B.9: (a) Temperature (upper panel), (b) salinity (lower panel) and (c) σ_t (lower panel) along Leg 11 from Tomczak and Pender (1998) as shown in Fig. B.1. The distance axis starts at the northernmost latitude.

At the western side of Tasmania (the zonal section at 42°S), the CARS atlas (Fig. B.10c) represents the deepening of the SML, although problems with the surface density field are still present. For the OCCAM climatology (Fig. B.11c), the deepening of the SML is more evident. Compared to the previous section (Figs. B.6 and B.8), the horizontal gradients of temperature and salinity are more reduced in both atlas. Comparisons with the same CTD data, but for Leg 12 (Fig. B.12), taken at around the same latitude of this section and between 141°E and 144.5°E shows a similar reduction of those horizontal gradients and a deepening of the SML close to the coast.

Lastly, for the section at the southern tip of Tasmania (146.5°E), both the CARS (Fig. B.13c) and OCCAM (Fig. B.14c) results show an offshore sinking of the isopycnals between 48°S and 50°S. Very close to the coast the OCCAM presents a further deepening of the isopycnals that does not occur in the CARS climatology. Comparisons with a CTD

cruise (Fig. 2.12) from Rintoul and Sokolov (1999) show that temperature and salinity isolines can sink down to 400 m between the coastal station and the latitude of 49°S. Due to the lack of a more coastal hydrographic stations, no further comparisons can be done in terms of further sinking of the isopycnals observed in OCCAM.

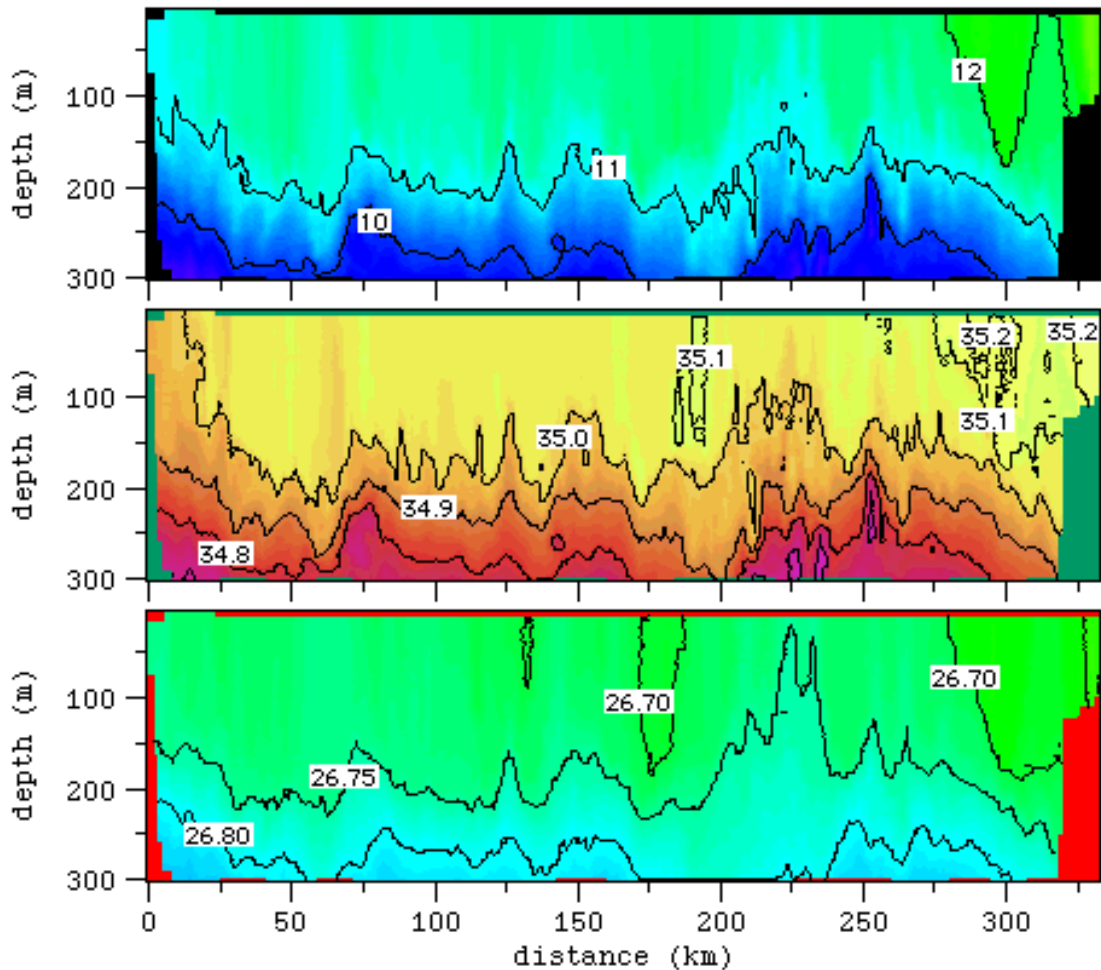


Figure B.12: Same as Fig. B.9, but along Leg 12. The distance axis starts at the westernmost latitude.

As an overall picture of the horizontal temperature and salinity distribution at the SEIO, plots at 10 m from CARS (Fig. 2.4) and 9 m from OCCAM (Fig. 2.5) were taken. In general terms, both show the penetration of the light and warm waters of the Leeuwin Current, the formation of a saltier water mass at the head of the GAB, with salinities up to 36.2 and also the tendency for a meridional distribution of the temperature and salinity gradients. What is not observed in OCCAM is that anomalous distribution of light water in front of Kangaroo Is.. OCCAM also seems to have a better resolved front for the East Australian Current.

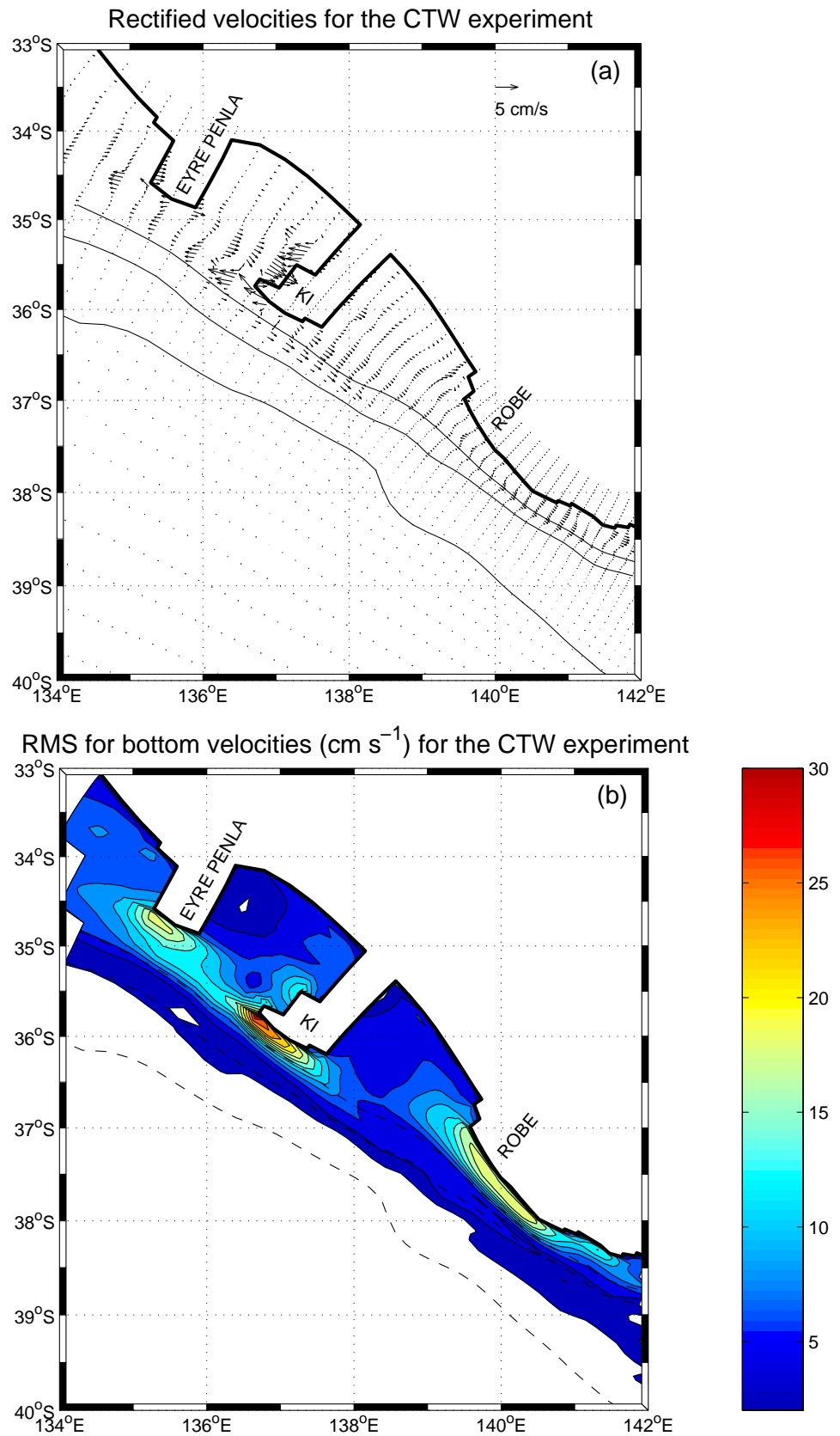


Figure D.2: (a) Residual velocity and (b) rms velocity at the bottom for the South Australian region described in Fig. 4.15. The contour interval is 2 cm s^{-1} . Solid (a) and dashed (b) lines are the 200, 1000 and 4000 m isobaths.

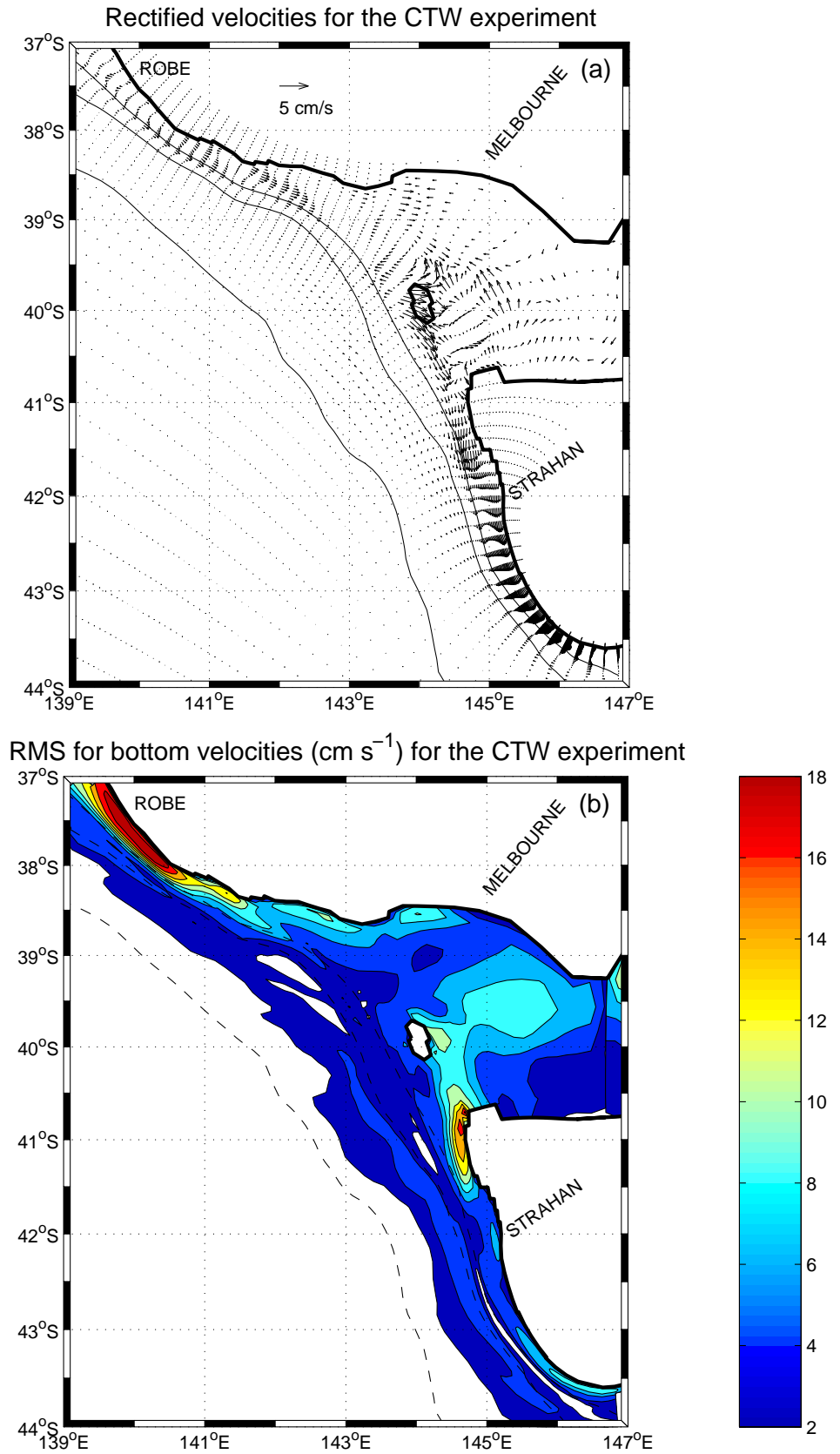


Figure D.3: Same as Fig. D.2, but for the Victoria-Tasmanian region.